Fabrication and Biocompatibility of Porously Bioactive Scaffold of Nonstoichiometric Apatite and Poly (ε-caprolactone) Nanocomposite

Liang Ye,[1] Xinchen Zeng,[2] Haojiang Li,[2] Zhe Wang[3]

[1]*Guanghua School of Stomatology, Sun Yat-sen University, Guangzhou 510080, People's Republic of China*
[2]*Zhongshan School of Medicine, Sun Yat-sen University, Guangzhou 510080, People's Republic of China*
[3]*School of Pharmaceutical Science, Sun Yat-sen University, Guangzhou 510080, People's Republic of China*

Received 3 May 2009; accepted 15 September 2009
DOI 10.1002/app.31466
Published online 10 December 2009 in Wiley InterScience (www.interscience.wiley.com).

ABSTRACT: Bioactive nanocomposite of nonstoichiometric apatite (ns-AP) and poly(ε-caprolactone) (PCL) was synthesized and its porous scaffold was fabricated. The results show that the hydrophilicity and cell attachment ratio on the composite surface improved with the increase of ns-AP content in PCL. The composite scaffolds with 60 wt % ns-AP content contained open and interconnected pores ranging in size from 200 to 500 μm and exhibit a porosity of around 80%. In addition, proliferation of MG_{63} cells on the composite scaffolds significantly increased with the increase of ns-AP content, and the level of alkaline phosphatase (ALP) activity and nitric oxide (NO) production of the cells cultured on the composite scaffold were higher than that of PCL at 7 days, revealing that the composite scaffolds had excellent *in vitro* biocompatibility and bioactivity. The composite scaffolds were implanted into rabbit mandible defects, the results suggest that the introduction of ns-AP into PCL enhanced the efficiency of new bone formation, and the ns-AP/PCL composite exhibited *in vivo* good biocompatibility and osteogenesis. © 2009 Wiley Periodicals, Inc. J Appl Polym Sci 116: 762–770, 2010

Key words: nonstoichiometric apatite; nanocomposite scaffold; cell response; osteogenesis; biocompatibility

INTRODUCTION

Hydroxyapatite (HA) bioactive ceramics as artificial bone have been extensively investigated and used in application in clinic for many years.[1–5] Recently, some studies have shown that nano hydroxyapatite (n-HA) had excellent performance and was a potential candidate of new biomaterials for tissue repair.[6,7] Nevertheless, the extensive use of n-HA is still limited by their powder state and brittle nature. Biodegradable polymers and their copolymers are widely used in bone regeneration, dental repair, orthopedic fixation devices, and many other biomedical applications.[8,9] It is known that pure polymers can not effectively bond to bone *in vivo* while bioactive materials do, such as HA.[10] Therefore, development of biocomposite of degradable polymer and bioactive inorganic material is still a promising approach to prepare bioactive implants for bone repair.[11]

Some studies suggested that the variation in the molar ratio of calcium to phosphate greatly affected the solubility of the Ca-P biomaterials,[12,13] and calcium phosphate with Ca/P of 1.50 degraded faster than hydroxyapatite with Ca/P of 1.67 when implanted *in vivo*.[14,15] Previous study showed that deficient calcium apatite also called nonstoichiometric apatite with Ca/P of 1.50 was biologically more active than pure HA ceramics alone because it has a composition and structure very close to natural bone mineral and therefore has been considered to be the ideal material for bone repair.[16] Thus, it is envisioned that nano nonstoichiometric apatite (ns-AP) for novel bone regeneration material can be fabricated in order to get better bioperformance of apatite biomaterial.

Biodegradable polymer, such as polycaprolactone (PCL) has attracted much interest because of its cost-efficiency, high toughness, and processibility resulting from its relatively low melting temperature. Also, a combination of PCL with bioactive inorganic materials could bring the advantages of both biomaterials. There have been a number of studies in the literature focusing on the composites created by combining biodegradable polymers and n-HA.[17,18] However, there were few previous reports about the preparation of ns-AP and PCL composite scaffolds as a bone repair material. It is expected that if the synthesis of ns-AP with degradability and bioactivity was used instead of HA, the degradability and bioactivity of the composites scaffold should be

Correspondence to: L. Ye (dentistyl@yahoo.cn or liangye456@yahoo.cn).

improved. Therefore, in this study, ns-AP/PCL composite scaffolds were prepared, and the biocompatibility and osteogenesis of the composite scaffolds were investigated.

MATERIALS AND METHODS

Synthesis of ns-AP

The ns-AP were synthesized using calcium nitrate ($Ca(NO_3)_2{\cdot}4H_2O$) and ammonium phosphate ($(NH_4)_2HPO_4$). First, calcium nitrate and ammonium phosphate (Ca/P mol ratio = 1.50, calcium nitrate: ammonium phosphate) were dissolved separately in deionized water. The calcium nitrate solution was dropped very slowly into the ammonium phosphate solution while stirring (300 r/min) at room temperature. The pH of the solution was kept between 10 and 12 by adding 24 wt % ammonium hydroxide. After the titration was completed, the mixture was set at room temperature for 24 h. The resulting apatite precipitate was washed with deionized water for five times, placed in a flask, and treated in deionized water for 2 h at 100°C. After treatment, the apatite precipitate consisted of ns-AP in slurry. The ns-AP slurry and dimethyl formamide (DMF) were mixed in a beaker while stirring, and the temperature was gradually increased 120°C. After all the water had evaporated, a mixture of ns-AP/DMF slurry was obtained. An aliquot was removed for transmission electron microscopy (FE-TEM, JEM-2100F, JEOL, Tokyo, Japan) testing. The value of Ca/P ratio of obtained ns-AP was measured by chemical titration.[19]

Preparation of ns-AP/PCL composite scaffolds

ns-AP/PCL composite scaffolds were prepared by solvent-casting and particulate leaching method. Briefly, 5 g PCL pellets (M_w = 80,000: Sigma-Aldrich Co, St. Louis, MO) were dissolved in 50 mL chloroform and 37.5 mL ns-AP/DFM slurry (concentration = 20% g/mL) was added to produce composites with 60 wt % ns-AP content. The mixture was stirred continuously for 2 h and then dried at 100°C for 4 h to remove the chloroform and part of the DMF. Sodium chloride (NaCl) was added as porogens (size: 300–450 μm; NaCl/PCL = 9/1,8/1,7/1,6/1,w/w), and the mixture was cast into Teflon molds containing 60 wells (each well: diameter, 10 mm; thickness, 5 mm). The samples were dried in a fume hood for 24 h to evaporate the DMF and were subsequently dried (vacuum) at 40°C for 48 h to remove any remaining solvent. To leach out the salt, the dry samples were immersed in deionized water for 36 h at room temperature, with water changes approximately every 6 h. The obtained scaffolds were dried in air for 24 h, the resulting porous scaffolds were stored in a desiccator until use. Using the same method, composite scaffolds with 40 wt %, 20 wt % and 0% ns-AP content were prepared. Composite scaffolds were made with different size by using different molds. For fabrication of dense samples, porogen of NaCl was not added into the composite.

Characterization of composite scaffolds

The phase composition of the ns-AP/PCL composite was examined by X-ray diffraction (XRD, Geigerflex, Rigaku, Japan) with Cu Kα radiation and Ni filter (λ =1.5406 A, 100 mA, 40 kV) in a continuous scan mode. The 2θ range was from 10 to 70° at a scanning speed of 10°/min. The surface morphology of the composite scaffolds was examined by scanning electron microscopy (FE-SEM, S-4300SE, Hitachi, Tokyo, Japan) at 2.0 kV. The dried specimens were glued onto copper specimen stubs, and sputter coated with gold before SEM observation. The porosity of the scaffolds was measured in distilled water by the Archimedes method.[20] The average porosity was calculated based on five samples.

The compressive strength of the composite scaffold samples (10 × 10 × 10 mm) was measured at room temperature using a compression test at a constant displacement rate of 2 mm/min. The jigs were specially designed to provide a uniform load on the composite samples, and a Bionix 858.20 (MTS Systems Corp. Eden Prairie, MN) was used to conduct tests. For each composition, three specimens were tested and the results were averaged.

Surface wettability of composite dense specimen sized 10 × 10 × 3 mm was determined by measuring the contact angle of water droplets on the surface of the various specimens using a contact angle measurement system (SEO 300A; Surface and Electro-Optics, Ansan, Korea). The water contact angle method was employed to determine polar interactions across the material-water interface. Each sample was mounted on the platform and a goniometer (Rame Hart, Mountain Lakes, NJ) was aligned and focused on the material-air interface. A microsyringe (Perfektum; Popper and Sons, Tokyo, Japan) was used to form 10 μL water droplets, which were dropped onto three different surface points on each sample; water contact angles were measured after 30 s. The results presented here represent the mean ± SD of four contact angles for per sample.

Cell attachment and proliferation

To investigate attachment and proliferation, composite dense samples with a size of 10 × 10 × 3 mm, were sonicated in ethanol and sterilized using ultraviolet light. For cell adhesion experiments, MG_{63}

cells were seeded on the disks at a density of 2×10^3 cells/disk. Cells were allowed to adhere for 1 h before each well was gently flooded with 1 mL of medium. Cell attachment was determined using a 3-(4,5-dimethylthiazol-2-yl)-2,5-diphenyltetrazolium bromide (MTT) assay after incubation for 4 h.

Cell proliferation was evaluated after seeding cells on the composite scaffolds with a size of Φ 10 $\times$ 5 mm at a density of 2×10^4 cells/scaffold, followed by incubation for 1, 3, and 5 days, with the medium replaced every second day. Adhesion and viable cells on substrates were assessed quantitatively using the MTT assay. In brief, composite scaffold-cell constructs were placed in a culture medium containing MTT and incubated in a humidified atmosphere at 37°C for 4 h. Cell growth was determined using the MTT assay (MTT Kit; Roche Diagnosis Corp., Indianapolis, IN). The absorbance value was measured at 570 nm using a microplate reader. Six specimens were tested at each incubation period, and each test was performed in triplicate. Results were reported as OD units.

Alkaline phosphatase activity and NO production

To evaluate alkaline phosphate (ALP) activity, 5×10^4 MG_{63} cells were seeded on the composite scaffolds with a size of Φ 10 $\times$ 5 mm, and ALP activity was measured after 1, 4, and 7. Before cell seeding, the scaffolds were soaked in 75% ethanol solution for 60 min and sterilized overnight under UV irradiation. The adherent cells were removed from composites and lysed with PBS (phosphate buffered saline); this procedure was followed by adding a cell lysis buffer containing 0.1% Triton X-100 to the samples and freezing them to −20°C. The frozen samples were thawed at 37°C for 5 min to measure ALP activity according to the manufacturer's instructions (ALP kit 104; Sigma). A 50-mL sample was mixed with 50 mL pNPP (*p*-nitrophenyl phosphate disodium, 1 mg/mL) in a 1 *M* diethanolamine buffer containing 0.5 m*M* $MgCl_2$ (pH 9.8) and incubated at 37°C for 15 min on a bench shaker. The reaction was stopped by adding 25 mL 0.1 *N* NaOH per 100 mL of reaction mixture. The number of cells was determined by measuring the DNA content using Quant-iT(tm) PicoGreen dsDNA reagent kits (Molecular Probes, Eugene, OR). Sample DNA was quantified by measuring fluorescence with a Synergy HT Multi-Detection Microplate Reader (BioTek, Winooski, VT) at wavelengths of 480 nm excitation and 520 nm emission. Enzyme activity was quantified by measuring absorbance at 405 nm, and ALP activity was calculated from a standard curve after normalizing to the total DNA content. The results are expressed in nanomoles of *p*-nitrophenol produced per minute per nanogram of DNA.

Osteoblast nitric oxide (NO) production was indirectly measured by cell supernatant nitrite quantification since it is a stable metabolite of NO. The Griess assay was used, according to manufacturer's protocol. Cells were cultured in the presence of the composite scaffolds for 7 days. Culture supernatant (50 μL) was mixed with reagent Griess Reagent I (50 μL) and Griess Reagent II (50 μL). After the sample was incubated for 20 min at room temperature, the absorbance was measured at 540 nm, and nitrite concentration was determined from a standard curve of serial dilutions of sodium nitrite dissolved in standard culture medium and normalized to protein in the cell culture supernatant.

Biocompatibility and osteogenesis *in vivo*

Biocompatibility and osteogenesis *in vivo* of the composite scaffolds were evaluated using macroscopic and histological methods. Briefly, the healthy New Zealand white rabbits weighing about 3.0 kg each were used for the implantation of the composite scaffolds. The rabbits were anesthetized with pentobarbital sodium. A 3-cm parallel incision was made on the jaw of the rabbit. The peristeum was retracted and the submaxilla was exposed. A critical size defect (10 $\times$ 6 $\times$ 3 mm) was made in buccal-lingual direction on one side of the mandible of each rabbit. 10 $\times$ 6 $\times$ 3 mm sized porous composite scaffolds were inserted into the defect and stabilized using fine stainless steel wires if necessary. Rabbits from each group were sacrificed at 4 and 12 weeks after implantation. The scaffolds together with surrounding tissue were excised, fixed in 10% neutral buffered formalin, decalcified and embedded in paraffin. Tissue blocks were sectioned to 4 μm in thickness and stained with Masson trichrome, and observed with light microscope (CX21, Olympus, Japan).

Statistical analysis

Statistical analysis was performed using one-way ANOVA with post hoc tests. All results are expressed as the mean ± standard deviation (SD). Differences were considered statistically significant at $P < 0.05$.

RESULTS

TEM and XRD analysis

Figure 1(a) shows a transmission electron micrograph of the ns-AP. It can be seen that the prepared ns-AP was rod-shaped with the size of 10–20 nm in diameter and 70–100 nm in length. The Ca/P ratio of the obtained ns-AP was 1.5 + 0.01. Figure 1(b)

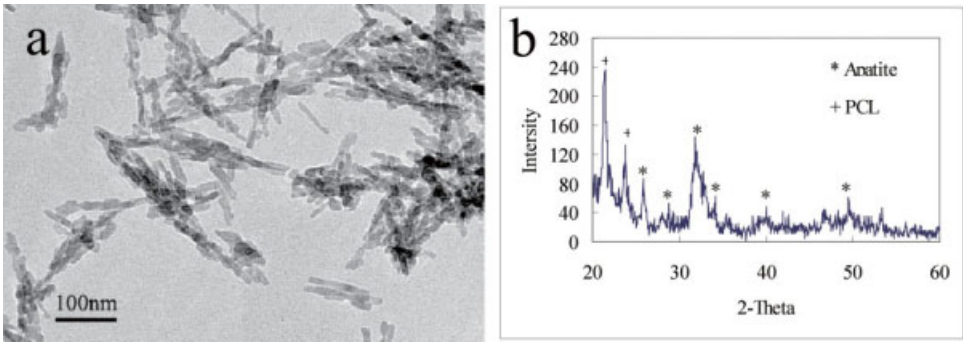

Figure 1 TEM photograph of (a) ns-AP, and XRD patterns of (b) ns-AP/PCL composite.

shows the XRD patterns of the ns-AP/PCL composite. It is found that the composite consisted of ns-AP and PCL phase, and the ns-AP presented apatite phase with low crystallinity, the peaks appeared at about 26, 29, 32, 33, 40, 49° [2θ], indicating that the apatite phase was present in the composite while the two peaks at about 21 and 23° [2θ] were assigned to PCL. No additional phase was identified within detectable limits.[21]

Hydrophilicity and cell attachment

Table I presents the water contact angles of the ns-AP/PCL composites. The table reveals that the water contact angles of the composite specimens significantly decreased with the increase of apatite content, indicating that the addition of apatite in PCL improved the hydrophilicity of the composites.

The MTT assay was used to assess the relative number of MG_{63} cells that adhered to the various biomaterials because optical density (OD) absorbance values can be used as indicators of the cells on the composites. Table I presents the results of cell attachment on the composite with different apatite content. After 4 h, the OD value of the composite with 60 wt % ns-AP was significantly higher than other composites and pure PCL ($P < 0.05$). These results indicate that cell attachment ratio increased with the ns-AP content, suggesting that the composites with high ns-AP content facilitated cell adhesion on their surfaces.

Morphology, porosity and compressive strength of composite scaffold

Figure 2 shows the surface morphology and microstructure of the composite porous scaffolds with 60 wt % ns-AP content under various magnifications, (a) × 50, (b) × 100, (c) × 500, and (d) × 20,000. The composite scaffold exhibited a macroporous structure with completely open and interconnected pores. By SEM, the pores appeared almost spherical in shape, with diameters of 200–500 μm shown in Figure 2(a,b). High-magnification SEM images further revealed that a number of small pores (1–10 μm) were distributed across the macropore walls shown in Figure 2(c). Examination at greater magnifications reveals that the composite scaffold surface exhibited typical spherical granules of apatite with the particles size of around 100 nm as shown in Figure 2(d). It can be seen that most apatites (arrow) were exposed on the composite surface except some ns-AP granules were embed in PCL matrix.

The porosity of the composite scaffolds with 60 wt % ns-AP prepared by this method was ranging from 61 to 82%, which increased with the increase of the amount of porogens (NaCl). The compressive strength of the composite scaffolds decreased with increasing porosity as shown in Table II. It can be seen that the compressive strength of the composite scaffold was 1.2 MPa as the porosity is 82%. The porosity was significantly affected by the amount of the porogens used in making the scaffolds.

Cell proliferation

Proliferation of MG_{63} osteoblast-like cells cultured on both the composite and PCL samples were assessed using the MTT assay because OD values can provide an indication of cell growth and proliferation on various biomaterials.[22] Figure 3 reveals that OD values for the composite with 60 wt % ns-AP were significantly higher than with 20 wt % ns-AP and PCL after 3 and 5 days ($P < 0.05$); no significant differences appeared after 1 day. These results indicate that cell growth and proliferation (after 3

TABLE I
Water Contact Angles and Cell Adhesion Rate on Composite and PCL

Samples	Water contact angle (°)	Cell attachment ratio (%)
PCL	77 ± 2.0	21.5 ± 2.0
1 (20 wt % ns-AP)	64.8 ± 1.5	30.4 ± 1.5
2 (40 wt % ns-AP)	40.0 ± 3.0	49.3 ± 2.0
3 (60 wt % ns-AP)	21.5 ± 1.0	56.8 ± 3

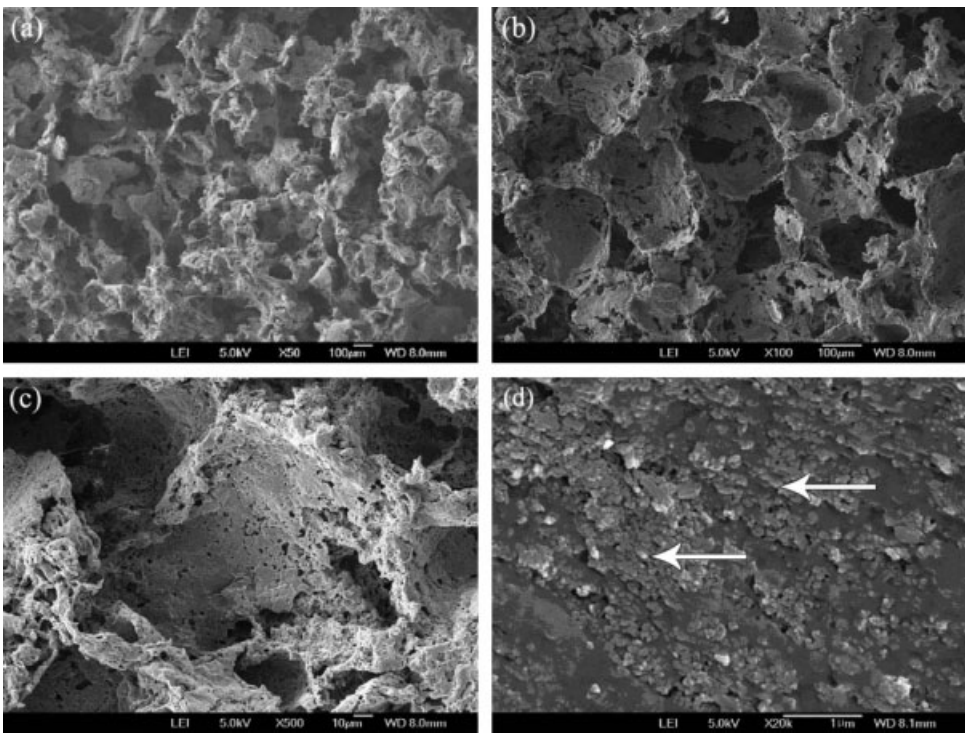

Figure 2 SEM photographs of the composite scaffolds with 60 wt % ns-AP at various magnification: (a) ×50, (b) ×100, (c) ×500, and (d) ×20,000, arrow represents ns-AP granules.

and 5 days) was superior in the composite with 60 wt % than 20 wt % ns-AP and PCL, suggesting that composite with 60 wt % ns-AP facilitated cell growth and could promote cell proliferation.

Cell differentiation

Cell differentiation was assessed in terms of testing ALP activity at 1, 4, and 7 days, as shown in Figure 4. At 1, 4 days respectively, ALP expressed at lower levels, and no significant differences were detected among composite with 60 wt %, 20 wt % ns-AP and PCL. Subsequently, ALP activity increased with time. Cells on the composites with 60 wt % and 20 wt % ns-AP exhibited higher levels of ALP activity at 7 days than at 4 days, indicating that cell differentiated most at 7 days. Moreover, at 7 days, ALP activity on the composite with 60 wt % was significantly greater than 20 wt % ns-AP and PCL samples ($P < 0.05$).

NO production of the osteoblast cultured on the composite scaffolds and PCL with time is shown in Figure 5. The results show that the ns-AP content in the composite had obviously effects on the NO production of osteoblasts. NO production level was significantly higher for the composite with 60 wt % compared with 20 wt % ns-AP and PCL ($P < 0.05$), indicating the composite with high ns-AP content caused higher NO production of cultured cells, and promoted cell differentiation.

Biocompatibility and osteogenesis *in vivo*

Macroscopic evaluation

Figure 6(a) shows the macroscopic evaluation of the composite samples implanted in the bone cavities of the rabbit mandibles for 4 weeks. The abscission of suture occurred at 4 weeks after operation. The wounds were cured well without dehiscence, and did not elicit any obvious inflammatory response in the adjacent soft tissue. Surface of bone defects were partially filled with callus bone. No signs of implant rejection, necrosis or infection were found at the experimental time. From X-ray microradiograph, it was found that the material/bone boundary became illegible at 4 weeks postimplantation, suggesting the occurrence of mineralization and increasing density of the implant [Fig. 6(b)]. The disappearance of the boundary between material and bone tissue at 4 weeks after implantation indicates that the density

TABLE II
Effects of Quantity of Porogens (NaCl) Used on Porosity and Compressive Strength of Composite Scaffolds with 60 wt % ns-AP

Specimens	PCL/NaCl (w/w)	Porosity (%)	Compressive strength (MPa)
1	1 : 9	82 ± 4	1.2 ± 0.8
2	1 : 8	77 ± 2	2.3 ± 1.0
3	1 : 7	68 ± 3	4.5 ± 1.4
4	1 : 6	61 ± 3	6.9 ± 1.2

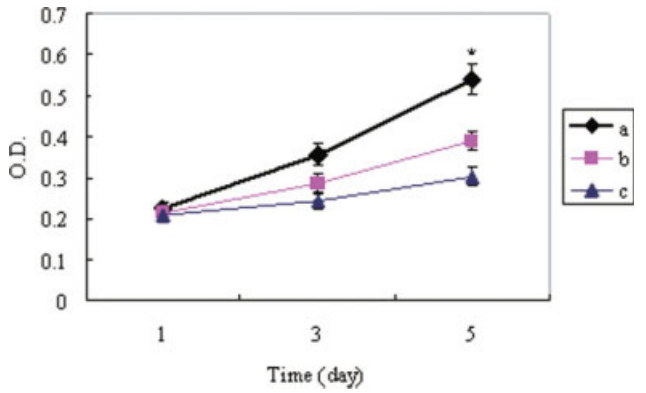

Figure 3 Proliferation of osteoblast on (a) 60 wt % and (b) 20 wt % ns-AP composite scaffolds with time ($n = 5$, $^*P < 0.05$), (c) PCL as a control. [Color figure can be viewed in the online issue, which is available at www.interscience.wiley.com.]

of newly formed bone was as high as that of host bone, and that a complete osteointegration between material and tissue has been achieved.

Histological evaluation

At 4 weeks after operation, no fibrous encapsulation was found while more newly formed bone tissues were found to deposit at the interface between the composite scaffold materials and bone tissue with the presence of active osteoblasts, and the amount of bone matrix were observed on the composite scaffolds to increase as shown in Figure 7(a). At 12 weeks, it was found that new bone regenerated and penetrated through the interconnected pores into the center of the composite scaffolds as shown in Figure 7(b). The boundary between scaffold material and host bone was unclear due to the sufficient amount of mature bone tissue that grew into the pores of the composite scaffold.

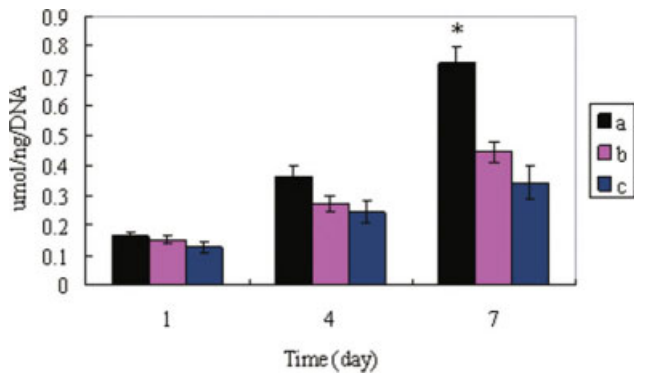

Figure 4 Alkaline phosphatase activity of osteoblast cultured on (a) 60 wt % and (b) 20 wt % ns-AP composite scaffolds with time ($n = 5$, $^*P < 0.05$), (c) PCL as a control. [Color figure can be viewed in the online issue, which is available at www.interscience.wiley.com.]

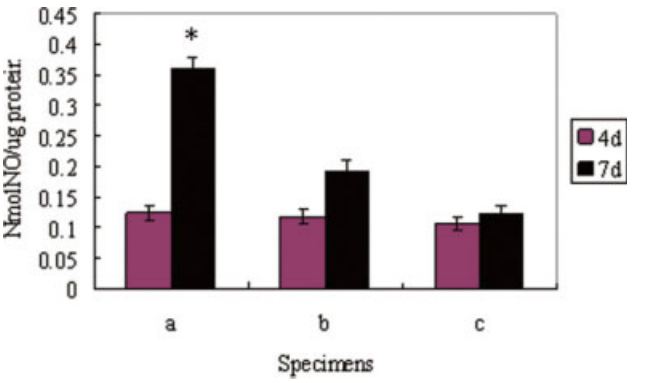

Figure 5 Nitric oxide production levels of osteoblast cultured on (a) 60 wt % and (b) 20 wt % ns-AP composite scaffolds with time ($n = 5$, $^*P < 0.05$), (c) PCL as a control. [Color figure can be viewed in the online issue, which is available at www.interscience.wiley.com.]

DISCUSSIONS

During the past few years, considerable effort has been spent on researching the nanostructure processing of nanoscale biomaterials and their biocomposites. Some studies have suggested that bioactive composites prepared at the nano-level could play important roles in various biomedical applications because of their unique functional properties, which could have a great impact on cell-biomaterial interactions.[23,24] A biocompatible porous scaffold is important as a temporary carrier for implanted cells in bone tissue engineering, and the scaffolds should have high levels of porosity, suitable pore size, and highly interconnected pore structure.[25] It was found that pores between 50 and 150 μm determine osteoid growth and pores larger than 150 μm facilitate cell proliferation, vascular ingrowth, and internal mineralized bone formation.[26] In this study, ns-AP/PCL bioactive nanocomposite porous scaffolds were fabricated by solvent-casting and particulate leaching method. These composite scaffolds exhibited a homogeneous distribution of open macropores and pore sizes mainly in the range of 200–500 μm, which was in accord with the size of the salt particles, and the porosity of scaffold increased with the increase of porogens (NaCl) content. Moreover, this study revealed that the composite scaffold has a good degree of interconnection. Therefore, the characteristic of the composite scaffolds is likely beneficial in facilitating cell infiltration and bone ingrowth.

The porosity of the composite scaffold had obvious effect on the compressive strength. The higher the porosity, the lower the compressive strength of the scaffold. The scaffolds exhibited the maximal porosity of 82%, with minimal compressive strength of 1.2 MPa. In addition, some larger pores resulting from porogens aggregation were observed,

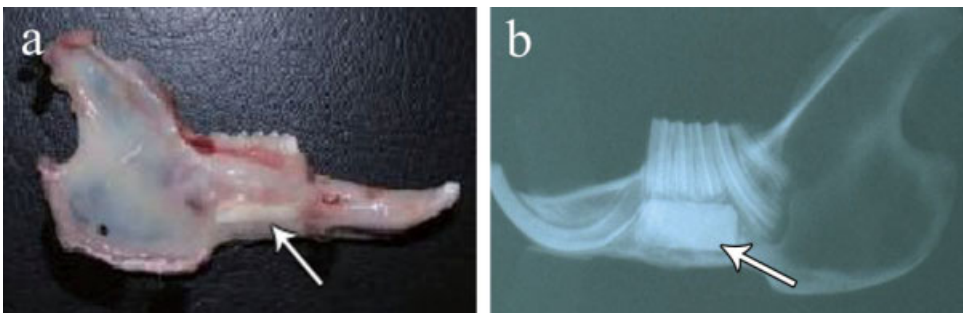

Figure 6 (a) Macroscopic evaluation and (b) X-ray microradiograph of samples implanted into bone defects of rabbits for 4 weeks, arrow represents composite scaffold with 60 wt % ns-AP. [Color figure can be viewed in the online issue, which is available at www.interscience.wiley.com.]

as well as some smaller pores created by scaffold shrinkage. Additional pores, with diameters between 1 and 10 μm, were dispersed on the macroporous walls of the scaffolds and may have been introduced during evaporation of the solvent; these pores might play important roles in nutrient diffusion. Yuan reported that micropores on the macroporous walls of a calcium phosphate ceramic were important in osteoinduction, and could induce bone formation.[27] Therefore, the small pores on the macroporous surface of the composite scaffolds may help improve the biological performance of the scaffolds.

Incorporating hydrophilic inorganic materials into hydrophobic polymers is a viable way to improve polymer hydrophilicity.[28] In present study, the results show that ns-AP into PCL markedly improved the hydrophilicity of the composites, and the values of the water contact angles depended on the ns-AP content because most of apatite was exposed on the composite surfaces. The higher the ns-AP content in PCL, the greater the hydrophilicity of the composite. Webb proposed that when biomaterial surfaces are exposed to dilute the serum, more hydrophilic surfaces are better for cell attachment, spreading, and proliferation than hydrophobic surfaces.[29] In addition, Yang et al. reported that a biomaterial's hydrophilicity aided absorption of fibronectin, which is essential for osteoblast adhesion *in vitro*.[30] Therefore, the composite's better hydrophilic surface might be suitable for cells attachment and proliferation.

Attachment is part of the first phase of cell-material interactions, and the quality of this first phase will influence the cell's capacity for growth, morphology, proliferation, and differentiation upon contact with the implant.[31] The cell attachment results of this study indicate that MG_{63} osteoblast-like cells adhered better to the composite with 60 wt % than 20 wt % ns-AP and PCL within the first 4 h. The superior ability of MG_{63} cells to attach to the composite with 60 wt % ns-AP is probably associated with differing material surface features between the composite and PCL. The nano-sized apatite exposed on the composite surfaces may have additional special surface properties as shown in Figure 2(d). which promote cell attachment, and the more hydrophilic surface of the composite may be more useful for cell adhesion than PCL. Moreover, the results also demonstrate that cell adhesion depended on the apatite content. The higher the ns-AP content in

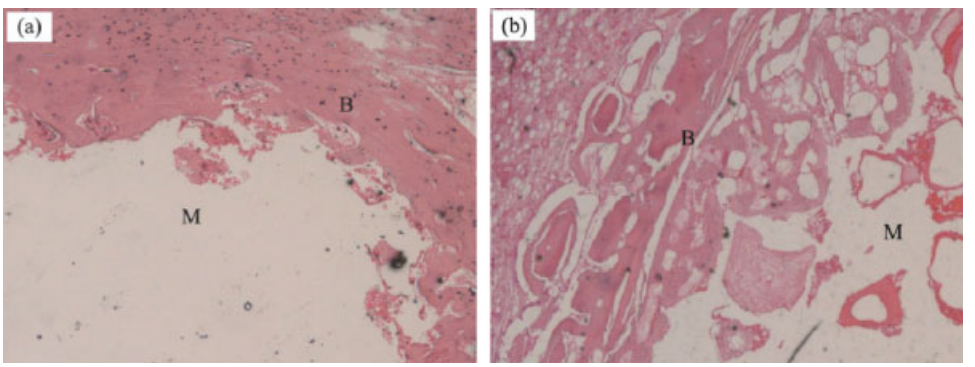

Figure 7 Histological photographs of rabbit mandible defect implanted with composite scaffolds with 60 wt % ns-AP for (a) 4 weeks and (b) 12 weeks, (H&E, 40×). In the photos, B denotes newly formed bone tissue (red), while M denotes scaffold materials. [Color figure can be viewed in the online issue, which is available at www.interscience.wiley.com.]

PCL, the more the apatite exposed on the composite surfaces, the greater the cell attached ratio.

Ideally, bioactive biomaterials need to interact actively with cells and stimulate growth. It was observed that the cells were able to proliferate on the composite scaffolds, as demonstrated by the MTT assay. Our results reveal that both the composite and PCL could stimulate the MG_{63} osteoblast-like cells growth and proliferation over time, and the cell proliferation on the composite scaffolds significantly depended on the apatite content. The higher the ns-AP content in PCL, the greater the ratio of cell proliferation. It is surmised that the composite surface features (ns-AP particles on the composite surfaces) might be responsible for stimulating cell growth and proliferation.

ALP activity has been used as an early marker for functionality and differentiation of osteoblasts during *in vitro* experiments.[32] In this study, ALP activity on the composite scaffolds with 60 wt % ns-AP exhibited significantly higher levels of expression than those on the composite with 20 wt % ns-AP and PCL at 7 days, indicating that cells differentiated more quickly after being cultured on the composite than on PCL. Therefore, the most distinct advantage the composite appears to be its superior ALP activity as compared to PCL. This increased activity probably resulted from the composite surface features, which might be responsible for stimulating cell differentiation.

NO is associated with the differentiation of osteoblasts cultured on the biomaterials.[33] The results show that ns-AP content in PCL had obvious effects on the NO production of osteoblasts. NO production level is significantly higher for the composite with 60 wt % compared to composite with 20 wt % ns-AP and PCL at 7 days, indicating high ns-AP content in PCL could promote cell differentiation. The differentiation of osteoblasts on the composite scaffolds also indicates good cell viability, suggesting good biocompatibility.

The results of *in vitro* experiments prompted us to investigate the bioproperties of the composite scaffold *in vivo*. A rabbit model (mandible defect) was used to investigate the hard tissue response to the composite scaffold in this study. During the experiment, all rabbits were healthy and did not show any wound complications. No inflammatory signs or adverse tissue reactions were found. To monitor the process of the formation of bone tissue, histological studies were performed on the composite specimens after different implantation periods. Active bone regeneration in the rabbit mandible defects was found in the composite scaffolds. Histological evaluation results show that the porous composite scaffolds by incorporation of ns-AP into PCL could be used as implants for bone regeneration. The results show that composite scaffolds presented not only good biocompatibility but also osteogenesis at the bone defect.

CONCLUSIONS

Nonstoichiometric apatite and poly(ε-caprolactone) nano bioactive composite was synthesized, and the fabricated composites had significantly greater hydrophilicity than PCL, which could support MG_{63} cell attachment. Porous scaffolds of the ns-AP/PCL composite with 60 wt % ns-AP content were prepared, and the scaffolds had a high porosity of around 82%, with open and interconnected pores ranging in size from 200 to 500 μm. Proliferation ratio of MG_{63} cells was significantly higher on the composite scaffolds with 60 wt % ns-AP than 20 wt % and PCL at 3 and 5 days, demonstrating the composite with higher apatite content can stimulate the cell proliferation. Furthermore, the level of ALP activity and NO production were obviously higher on the composite with 60 wt % ns-AP than 20 wt % and PCL after 7 days, revealing that increase apatite content in composite can promote the cells differentiation. The results confirm that the ns-AP/PCL biocomposite scaffolds showed good *in vitro* biocompatibility. Histological evaluation results demonstrated that composite with 60 wt % ns-AP implants exhibited efficiency of bone regeneration. The prepared composite scaffolds could be applied as bioactive bone implants that might stimulate tissue regeneration.

The authors thank Ms. Fan Minghui from Institute of Chemistry and Materials Science, University of Science and Technology of China for her assistance in material preparation of this article.

References

1. Best, S. M.; Porter, A. E.; Thian, E. S.; Huang, J. J Eur Ceram Soc 2008, 7, 1319.
2. Sun, J. S.; Liu, H. C.; Chang, H. S.; Li, J.; Lin, F. H.; Tai, H. C. J Biomed Mater Res 1998, 39, 390.
3. Willmann, G. Adv Eng Mater 1999, 1, 95.
4. Kokubo, T.; Kim, H. M.; Kawashita, M.; Nakamura, T. J Mater Sci Mater Med 2004, 15, 99.
5. Hedia, H. S. J Biomed Mater Res B 2005, 75, 74.
6. Shor, L.; Guceri, S.; Wen, X. J.; Gandhi, M.; Sun, W. Biomaterials 2007, 28, 5291.
7. Sachlos, E.; Gotora, D.; Czernuszka, J. T. Tissue Eng 2006, 9, 2479.
8. Waris, E.; Ashammakhi, N.; Lehtimäki, M.; Tulamo, R.-M.; Törmälä, P.; Kellomäki, M.; Tormala, P.; Konttinen, Y. T. Biomaterials 2008, 29, 2509.
9. Owen, G. R.; Jackson, J.; Chehroudi, B.; Burt, H.; Brunette, D. M. Biomaterials 2005, 26, 7447.
10. Nukavarapu, S. P.; Kumbar, S. G.; Brown, J. L.; Krogman, N. R.; Weikel, A. L.; Hindenlang, M. D. Biomacromolecules 2008, 7, 1818.

11. Hong, Z.; Zhang, P.; He, C.; Qiu, X.; Liu, A.; Chen, L. Biomaterials 2005, 32, 6296.
12. Tenhuisen, K. S.; Brown, P. W. J Biomed Mater Res 1997, 36, 233.
13. Liu, C.; Shen, W.; Chen, J. Mater Chem Phys 1999, 58, 78.
14. Kannan, S.; Pina, S.; Ferreira, J. M. F. J Am Ceram Soc 2006, 10, 3277.
15. Fulmer, M. T.; Ison, I. C.; Hankermayer, C. R.; Constantz, B. R.; Ross, J. Biomaterials 2002, 23, 751.
16. Aizawa, M.; Ueno, H.; Itatani, K.; Okada, I. J Eur Ceram Soc 2006, 4, 501.
17. Huang, Y. X.; Ren, J.; Chen, C.; Ren, T. B.; Zhou, X. Y. J Biomater Appl 2008, 5, 409.
18. Zhou, D. S.; Zhao, K. B.; Li, Y.; Cui, F. Z.; Lee, I. S. J Bioact Compat Polym 2006, 5, 373.
19. Liu, C.; Huang, Y.; Shen, W.; Cui, J. Biomaterials 2001, 22, 301.
20. Guo, H.; Su, J. C.; Wei, J.; Kong, H.; Liu, C. S. Acta Biomaterialla 2009, 5, 268.
21. Li, Y.; Zhang, X.; De Groot, K. Biomaterials 1997, 18, 737.
22. Von, W. C.; Vairaktaris, E.; Pohle, D.; Rechtenwald, T.; Lutz, R.; Münstedt, H.; Koller, G.; Schmidt, M.; Neukam, F. W.; Schlegel, K. A.; Nkenke, E. J Biomed Mater Res A 2008, 87, 896.
23. Tanaka, T.; Hirose, M.; Kotobuki, N.; Ohgushi, H.; Furuzono, T.; Sato, J. Mater Sci Eng C 2007, 4, 817.
24. Zhu, X.; Eibl, O.; Scheideler, L.; Geis-Gerstorfer, J. J Biomed Mater Res A 2006, 1, 114.
25. Mobini, S.; Javadpour, J.; Hosseinalipour, M.; Ghazi-Khansari, M.; Khavandi, A.; Rezaie, H. R. Adv Appl Ceram 2008, 1, 4.
26. Nejati, E.; Mirzadeh, H.; Zandi, M. Compos Part A-Appl S 2008, 39, 1589.
27. Yuan, H.; Kurashina, K.; De, Groot, K.; Zhang, X. Biomaterials 1999, 20, 1799.
28. Ho, M. L.; Fu, Y. C.; Wang, G. J.; Chen, H. T.; Chang, J. K.; Tsai, T. H.; Wang, C. K. J Controlled Release 2008, 128, 142.
29. Webb, K.; Hlady, P. A. J Biomed Mater Res 1998, 41, 422.
30. Yang, M.; Zhu, S.; Chen, Y.; Chen, G.; Gong, Y. Biomaterials 2004, 25, 1365.
31. Xuanyong, L.; Chuanxian, D. Surf Coat Tech 2003, 172, 270.
32. Hongli, S.; Chengtie, W.; Kerong, D.; Jiang, C.; Tingting, T. Biomaterials 2006, 27, 5651.
33. In, J. S.; Kim, S. Y.; Cho, S. K.; Chong, M. S.; Kim, K. S. Biomaterials 2007, 28, 1115.